

Analysis of On-policy Policy Gradient Methods under the Distribution Mismatch

Weizhen Wang, Jianping He, Xiaoming Duan

Abstract—Policy gradient methods are one of the most successful methods for solving challenging reinforcement learning problems. However, despite their empirical successes, many SOTA policy gradient algorithms for discounted problems deviate from the theoretical policy gradient theorem due to the existence of a distribution mismatch. In this work, we analyze the impact of this mismatch on the policy gradient methods. Specifically, we first show that in the case of tabular parameterizations, the methods under the mismatch remain globally optimal. Then, we extend this analysis to more general parameterizations by leveraging the theory of biased stochastic gradient descent. Our findings offer new insights into the robustness of policy gradient methods as well as the gap between theoretical foundations and practical implementations.

I. INTRODUCTION

The policy gradient (PG) algorithms are designed to identify the best parameterized policy that optimizes a performance metric by iteratively updating parameters along the gradient direction. In reinforcement learning (RL), popular PG methods, such as TRPO [1], A3C [2], GAE [3], PPO [4], SAC [5] are widely used to maximize a discounted accumulative reward and have demonstrated strong empirical performance. Since the policy gradient is an expectation with respect to the state distribution, sampling is commonly employed to accelerate the training process. However, as noted by [6], there exists a discrepancy between the practical sampling distribution and the true state distribution given by the theory.

This distribution mismatch introduces bias in gradient estimates, making many SOTA PG algorithms effectively biased stochastic gradient methods. Despite their impressive empirical success, these biased updates lack a rigorous theoretical foundation and can result in arbitrarily suboptimal performance in certain settings [7]. Nevertheless, due to their ease of implementation and strong empirical performance, biased PG algorithms remain widely adopted, and the impact of this distribution mismatch is often overlooked. A typical on-policy PG algorithm estimates the gradient by sampling state-action pairs according to the current policy, storing the data in a buffer, and then calculating a gradient estimate using minibatch data uniformly sampled from the buffer. However,

since the true theoretical state distribution is temporally discounted and practically inaccessible, a persistent distribution mismatch arises. Thus, it is crucial to analyze its impact and assess the robustness of this class of on-policy algorithms.

Related work: The state distribution mismatch has been highlighted in numerous studies [6]–[12] and it is particularly problematic as it can lead to arbitrarily suboptimal performance in certain scenarios. When it comes to correcting the bias, existing methods typically introduce significant computational and design complexity. Zhang et al. [8] consider this bias in *episodic* setting and take advantage of the equivalent temporal formulation of the gradient derived in [7]. Since the bias of the spatial distribution can be attributed to the absence of discount factor γ^t in step t , they propose the DisPPO algorithm which reintroduces the reweighting factor, γ^t , to each state-action pair (S_t, A_t) . However, this approach requires labeling all samples chronologically, causing data points appearing later in a trajectory to contribute exponentially less to the gradient update. This limitation can affect the effectiveness of leveraging distant samples for policy optimization. Since the bias arises from a distribution shift, another common approach to addressing it is importance sampling. Che et al. [11] focus on the *continuing* setting and introduce an averaging correction factor that theoretically corresponds to the importance ratio. To approximate this ratio in practice, they propose a buffer-based approach, where data is collected in a replay buffer with timestamps recorded during the sampling process. An auxiliary neural network is then trained via regression to estimate the correction ratio. While this correction improves the final policies compared to biased algorithms and disPPO [8] in several problems, it introduces additional computational overhead. Furthermore, their experimental results indicate that biased algorithms still outperform the corrected ones in certain scenarios.

On the other hand, instead of correcting the distribution, Tosatto et al. [10] derive an alternative formulation of policy gradient that avoids the discounted distribution by connecting it with the gradient of the action value function $\nabla_{\theta} Q^{\pi}$, which they refer to as the gradient critic. If both the action value function Q^{π} and the gradient critic $\nabla_{\theta} Q^{\pi}$ are known, then an exact policy gradient can be computed by averaging over the initial state distribution, thereby avoiding reliance on the inaccessible state distribution. They further demonstrate that the gradient critic satisfies a Bellman equation, allowing its estimation through well-established temporal-difference algorithms. However, despite its theoretical advantages, this approach still introduces additional computational costs and estimation error.

This work was supported in part by the Natural Science Foundation of Shanghai under Grant 23ZR1428900 and the National Natural Science Foundation of China under Grant 62373247 and 62303314.

The authors are with the Department of Automation, Shanghai Jiao Tong University, and Key Laboratory of System Control and Information Processing, Ministry of Education of China, Shanghai, China. Email: wangwz.im@gmail.com, {jphe, xduan}@sjtu.edu.cn.

Pan et al. [12] investigate several heuristic bias rectification approaches through extensive experiments, but their work does not provide theoretical insights. Notably, in some of these studies, experimental results suggest that the performance of the corrected algorithms can even be worse than that of the original, uncorrected algorithms. This further emphasizes the need for a deeper theoretical analysis of the robustness of biased policy gradients.

Although various correction methods have been proposed to address the distribution mismatch in policy gradient algorithms, they often introduce significant computational complexity and, in some cases, even underperform compared to biased methods. As a result, biased policy gradient algorithms remain the dominant choice in practical applications. However, the theoretical foundations of these algorithms remain underexplored, and their remarkable empirical performance in practical applications has also yet to be thoroughly explained. To address these gaps, this paper investigates the theoretical properties and practical performance of biased policy gradient methods.

Contributions: In this paper, we investigate the theoretical and practical implications of distribution mismatch in on-policy policy gradient methods for discounted RL problems. Our main contributions are summarized as follows:

- **Theoretical analysis for tabular parameterizations.** Focusing on tabular parameterizations, which serve as a foundational setting for analyzing convergence and optimality in reinforcement learning, we prove that distribution shift does not hinder global optimality. Our results establish that biased policy gradient methods can still attain optimal solutions under tabular policies.
- **Convergence bounds for general parameterizations.** We extend our analysis to more general parameterizations by deriving a discrepancy bound between the biased and unbiased distributions, which depends on the discount factor γ . Importantly, as γ approaches 1, the distribution mismatch diminishes. Under mild assumptions, we derive a convergence bound for the biased gradient algorithm.

II. BACKGROUND

A. Policy gradient methods

Markov decision process: We consider a finite Markov decision process (MDP) $M = \langle \mathcal{S}, \mathcal{A}, \mathcal{R}, p, \gamma, d_0 \rangle$, where \mathcal{S}, \mathcal{A} represent the state and action spaces, respectively, $R(s, a) \in \mathcal{R}$ denotes the expected reward for a given state-action pair (s, a) , the state transition probability $p(s' | s, a)$ describes the likelihood of transitioning into state s' from state s when taking action a , $\gamma \in [0, 1)$ is the discount factor determining the relative importance of future rewards and d_0 is the initial state distribution. We assume that rewards are bounded for all state-action pairs, i.e., $R(s, a) \in [-R_{\max}, R_{\max}]$ for all $s \in \mathcal{S}$ and $a \in \mathcal{A}$.

Policy and performance metric: Given a policy $\pi : \mathcal{S} \times \mathcal{A} \rightarrow [0, 1]$, $\pi(a | s)$ denotes the probability of taking action a at state s . The objective of RL is to learn an optimal policy

to optimize a performance metric. One common objective function $J(\pi)$ is the expected discounted return when the agent starts from an initial state s_0 sampled according to d_0 and follows a policy π : $J(\pi) \triangleq \mathbb{E}_\pi [\sum_{t=0}^{\infty} \gamma^t R_t]$. The state value function $V^\pi(s)$ quantifies the expected discounted return when starting from state $s \in \mathcal{S}$ and subsequently executing policy π : $V^\pi(s) \triangleq \mathbb{E}_\pi [\sum_{t=0}^{\infty} \gamma^t R_t | s]$. Similarly, the state-action value functions, denoted by Q^π , represents the expected discounted reward from a given state-action pair $(s, a) \in \mathcal{S} \times \mathcal{A}$: $Q^\pi \triangleq \mathbb{E}_\pi [\sum_{t=0}^{\infty} \gamma^t R_t | s, a]$. Using these definitions, the objective function $J(\pi)$ can also be expressed as the expected state value under the initial state distribution: $J(\pi) = \sum_s d_0(s) V^\pi(s)$ [13]. Our analysis considers both continuing and episodic MDPs. Without loss of generality, we assume the episodic MDP contains a single absorbing state z and the agent eventually reaches z under any policy. In this absorbing state, we have $p(z | z, \cdot) = 1$, $R(z, \cdot) = 0$ and thus $V^\pi(z) = 0$. We also assume $d_0(z) = 0$, and it does not affect the optimal policy since $V^\pi(z) = 0$. To ensure adequate exploration, we assume $d_0(s) > 0$ for all transient states s , following similar assumptions in [14], [15]. When π is fixed, the MDP has an associated Markov chain with a transition matrix P^π and $P^\pi(s' | s) = \mathbb{E}_{a \sim \pi(\cdot | s)} [p(s' | s, a)]$.

Policy gradient: When there are a large number of states and actions, an effective approach to representing the policy is to use a parameterized function π_θ . We slightly abuse the notation by writing $J(\theta)$ as a shorthand for $J(\pi_\theta)$. Gradient-based methods can then be employed to iteratively approach an optimal solution by updating the parameters as $\theta_{t+1} = \theta_t + \eta \nabla_\theta J(\theta_t)$, where η is the step size. Sutton et al. [16] derive the policy gradient formula as follows:

$$\nabla_\theta J(\theta) = \sum_{s \in \mathcal{S}} \mu_\pi(s) \sum_{a \in \mathcal{A}} \nabla_\theta \pi(a | s) Q^\pi(s, a), \quad (1)$$

where μ is the discounted state visitation counts defined by

$$\mu_\pi(s) = \sum_{t=0}^{\infty} \mathbb{E}_{s_0 \sim d_0} \gamma^t [P^\pi(s_t = s | s_0)]. \quad (2)$$

B. Distribution mismatch

The policy gradient (1) provides a compact spatial representation that has led to the development of a range of efficient policy gradient algorithms. However, in cases where the MDP model is unknown, the discounted state visitation counts μ_π in (2) becomes intractable to obtain. Additionally, in problems with large state and action spaces, the summation in (1) is also impractical. To address these issues, the policy gradient is often reformulated in its expectation form:

$$\nabla_\theta J \propto \mathbb{E}_{s \sim d_{\pi, \gamma}, a \sim \pi(\cdot | s)} [\nabla_\theta \ln \pi(a | s) Q^\pi(s, a)] \triangleq \nabla_\theta^\circ J, \quad (3)$$

where $d_{\pi, \gamma}$ is a valid probability distribution. In continuing tasks, $d_{\pi, \gamma}$ is the normalized version of μ_π , obtained by scaling μ_π by a factor of $1 - \gamma$. For episodic MDPs, $d_{\pi, \gamma}$ is constructed by setting $\mu_\pi(z) = 0$ and normalizing the remaining elements of μ_π , which is theoretically sound since $Q^\pi(z, \cdot) = 0$. The reformulated policy gradient $\nabla_\theta^\circ J$ in (3)

Algorithm 1 Sampling data into buffer

Input: initial distribution d_0 , current policy π
Initialize replay buffer \mathcal{B} with capacity C_0
while $|\mathcal{B}| < C_0$ **do**
 Start with initial state $S_0 \sim d_0$
 for time step $t = 0, 1, \dots$ **do**
 Take action $A_t \sim \pi(\cdot | S_t)$, observe R_t, S_{t+1}
 Store (S_t, A_t, R_t, S_{t+1}) in the buffer \mathcal{B}
 if S_{t+1} is an absorbing state **then**
 Break
 end if
 end for
end while

is widely adopted in practical algorithms since it enables the use of sampling-based methods to efficiently approximate the policy gradient, where the normalization constant can be treated as being absorbed by the stepsize [17]. This approach makes it computationally feasible to compute the policy gradient and is thus a cornerstone of policy gradient methods based on the stochastic gradient descent.

Nevertheless, as $d_{\pi, \gamma}$ is not directly accessible in practical sampling, a distribution mismatch arises in many implementations. More specifically, modern on-policy reinforcement learning algorithms, such as the most successful PPO [4], use a buffer to store the experience data and later sample from this buffer to form various estimates. As shown in Algorithm 1, during training, state-action pairs from trajectories are stored in a buffer. Each trajectory typically starts from an initial state $s_0 \sim d_0$, and as the policy π is executed, subsequent states and actions are recorded. As the buffer size grows, the frequencies of states within the buffer converges to the undiscounted state distribution d_π . Specifically: In continuing tasks, d_π is the stationary distribution of the current transition matrix P^π . In episodic tasks, $d_\pi(z) \triangleq 0$ for the terminal state z , while for a transient state s , $d_\pi(s)$ is proportional to the cumulative state visitation counts $\sum_{t=0}^{\infty} \mathbb{E}_{s_0 \sim d_0} [P^\pi(s_t = s | s_0)]$ and d_π is normalized to sum to 1 (as detailed in (13)). As a result, the state distribution estimated from buffer samples is biased towards d_π , leading to the following biased policy gradient:

$$\hat{\nabla}_\theta^\epsilon J \triangleq \mathbb{E}_{s \sim d_\pi, a \sim \pi(\cdot | s)} [\nabla_\theta \ln \pi(a | s) Q^\pi(s, a)]. \quad (4)$$

Consequently, policy gradient algorithms actually execute biased updates of the form:

$$\theta_{t+1} = \theta_t + \eta \hat{\nabla}_\theta^\epsilon J(\theta_t). \quad (5)$$

III. MAIN RESULTS

In this section, we aim to better understand biased policy gradient methods for their robust performance. The proofs for the theoretical results are provided in the appendices.

A. Tabular policy parameterization

We begin our analysis by examining two simple but widely studied tabular parameterization approaches: direct parameterization and tabular softmax parameterization, where for

any state-action pair $(s, a) \in \mathcal{S} \times \mathcal{A}$, a parameter $\theta_{s,a}$ describes the action probability. Owing to their simplicity, these two formulations have served as foundational models for deriving theoretical insights into policy gradient methods [14], [15], [18], [19] and continue to inspire subsequent research. The detailed proofs of this subsection are provided in Appendix I.

Direct parameterization: Under the direct parameterization, each state-action probability is determined by $\pi_\theta(a | s) = \theta_{s,a}$. For the biased gradient in (4), the corresponding component for (s, a) can be written as

$$(\hat{\nabla}_\theta^\epsilon J)_{(s,a)} = d_\pi(s) Q^\pi(s, a), \quad (6)$$

where $(\hat{\nabla}_\theta^\epsilon J)_{(s,a)}$ denotes the entry of the gradient associated with the state-action pair (s, a) . We show that this structure induces a gradient domination property with respect to the biased gradient $\hat{\nabla}_\theta^\epsilon J$.

Theorem 1 (Gradient domination): For the direct policy parameterization, let J^* and π_* denote the optimal objective value and an optimal policy, respectively. Then, for any policy π ,

$$J^* - J(\pi) \leq \kappa \left\| \frac{d_{\pi_*, \gamma}}{d_\pi} \right\|_\infty \max_{\bar{\pi}} (\bar{\pi} - \pi)^\top \hat{\nabla}_\theta^\epsilon J(\pi).$$

Here, $\kappa = \frac{1}{1-\gamma}$ in the continuing setting, and in episodic tasks, κ is a scale factor associated with π_* .

The property in Theorem 1 establishes the global optimality of the first-order stationary point for the biased policy gradient. Consequently, even though the gradient is biased, it still leads to an optimal solution.

Tabular softmax parameterization: The tabular softmax policies characterize the probability of selecting a state-action (s, a) by $\pi_\theta(a | s) = \frac{\exp(\theta_{s,a})}{\sum_{a' \in \mathcal{A}} \exp(\theta_{s,a'})}$. Its biased gradient is then given by

$$(\hat{\nabla}_\theta^\epsilon J)_{(s,a)} = d_{\pi, \gamma}(s) \pi(a | s) A^\pi(s, a), \quad (7)$$

where $A^\pi(s, a)$ is the advantage function under policy π . We establish that with tabular softmax parameterizations, biased policy gradient methods can still attain asymptotic global convergence, just as the behavior of the exact gradient studied in [15].

Theorem 2 (Global convergence): For the tabular softmax parameterization, by following iterates θ_t of the biased PG method in (5) with stepsize $\eta \leq \frac{(1-\gamma)^2}{8}$, π_{θ_t} converges asymptotically to an optimal solution π_* .

Results in Theorem 1 and Theorem 2 illustrate that even in the presence of the distribution mismatch, biased gradients still retain key theoretical guarantees for global convergence in tabular policy settings. This insight sets the stage for extending the analysis to more complex parameterizations and underscores the practical robustness of biased policy gradient methods.

Remark 1 (Convergence under general parameterizations): In fact, global optimality is not limited to the tabular parameterization where all possible policies can be represented. In some problems, although the

parameterization has limited representation capabilities, the biased gradient methods can still achieve global optimality in the policy class that is representable. Interestingly, the biased gradient may even demonstrate faster convergence compared to the exact unbiased gradient. An illustrative example is provided in Appendix I.3.

B. Bounds for distribution mismatch

We now extend our analysis beyond tabular settings to more general parameterizations. First, we focus on deriving theoretical bounds that quantify the distribution mismatch, which will be useful for characterizing the discrepancy between $\nabla_{\theta}^e J$ and $\hat{\nabla}_{\theta}^e J$. While Wu et al. [9] also attempt to quantify the error arising from the mismatch, their analysis focuses on the distance between the biased and unbiased *unnormalized* state visitation counts μ_{π} in (2) and use a different distance metric.

Episodic MDPs: In the episodic MDP setting, given a policy π , let \tilde{P}^{π} denote the principal minor of P^{π} restricted to the transient states and \tilde{P}^{π} is a row-substochastic matrix. The discounted and undiscounted state distributions over the transient states are denoted by $\tilde{d}_{\pi,\gamma}$ and \tilde{d}_{π} , respectively, which are well-defined probability distributions since $d_{\pi,\gamma}(z) = d_{\pi}(z) = 0$. We adopt the following standard assumption on the absorbing probability [9]:

Assumption 1 (Absorbing probability): There exists an integer $m > 0$ and a positive real number $0 \leq \alpha < 1$ such that $\mathbb{P}(s_m \neq z | s_0, \pi) \leq \alpha, \forall s_0 \in \mathcal{S}, \pi$.

Based on Assumption 1, we have the following bounds.

Theorem 3 (Mismatch bound for episodic MDPs):

Under Assumption 1, the infinity norm of the pointwise ratio between the discounted and undiscounted distributions $\tilde{d}_{\pi,\gamma}, \tilde{d}_{\pi}$ is bounded by

$$\left\| \frac{\tilde{d}_{\pi,\gamma}}{\tilde{d}_{\pi}} \right\|_{\infty} \leq \frac{1 - \alpha\gamma^m}{\gamma^{m-1}(1 - \alpha)}, \quad (8)$$

$$\left\| \frac{\tilde{d}_{\pi}}{\tilde{d}_{\pi,\gamma}} \right\|_{\infty} \leq \gamma + \frac{m(1 - \gamma^m)}{(1 - \alpha)(1 - \alpha\gamma^m) \min_s d_0(s)}. \quad (9)$$

Continuing MDPs: In the continuing MDP setting, the undiscounted distribution d_{π} corresponds to the stationary distribution of the transition matrix P^{π} . Similar to Che et al. [11], we assume ergodicity for the Markov chains associated with all policies:

Assumption 2 (Ergodicity): Given any policy π , the corresponding Markov chain P^{π} is ergodic.

By Assumption 2, each P^{π} is irreducible and $d_{\pi}(s) > 0$ for all any state s . Furthermore, since $d_{\pi,\gamma} \geq (1 - \gamma)d_0$, we also have $d_{\pi,\gamma}(s) > 0$ for all feasible policies π . We further assume a strictly positive lower bound across the entire policy class for the state distribution as follows:

Assumption 3 (Positiveness): For all feasible policies π , $c_{\min,\gamma} = \inf_{\pi,s} d_{\pi,\gamma}(s) > 0$ and $c_{\min} = \inf_{\pi,s} d_{\pi}(s) > 0$.

Given these assumptions, we derive the following bounds:

Theorem 4 (Mismatch bound for continuing MDPs):

Under Assumption 2 and Assumption 3, there exist constants $\beta \in (0, 1)$ and $D > 0$ such that the infinity

norm of the pointwise ratio between the discounted and undiscounted state distributions $d_{\pi,\gamma}, d_{\pi}$ satisfies:

$$\left\| \frac{d_{\pi,\gamma}}{d_{\pi}} \right\|_{\infty} \leq 1 + \frac{2(1 - \gamma)D}{(1 - \gamma\beta)c_{\min}}, \quad (10)$$

$$\left\| \frac{d_{\pi}}{d_{\pi,\gamma}} \right\|_{\infty} \leq 1 + \frac{2(1 - \gamma)D}{(1 - \gamma\beta)c_{\min,\gamma}}. \quad (11)$$

The proof of Theorem 3 and Theorem 4 are postponed to Appendix II. It is noteworthy that as γ approaches 1, the bounds in Theorem 3 and Theorem 4 converge to 1, effectively eliminating the distribution mismatch. Actually, in practical implementations of policy gradient algorithms, γ is typically chosen to be very close to 1 (e.g., 0.99 or 0.995) to prioritize long-term rewards while maintaining numerical stability. This choice naturally keeps the distribution mismatch relatively small, thereby ensuring that the biased gradient $\hat{\nabla}_{\theta}^e J$ performs comparably to its unbiased counterpart $\nabla_{\theta}^e J$.

C. Convergence of biased PG

Building on mismatch bounds derived in the last subsection, we next investigate the convergence properties of biased policy gradient methods with less restrictive parameterizations. Intuitively, if the mismatch remains small, biased gradients should achieve performance comparable to that of the unbiased gradient. We assume the following.

Assumption 4 (Parameterization assumption): For all $(s, a) \in \mathcal{S} \times \mathcal{A}$ and θ , the following conditions hold:

- **Bounded gradient:** The policy gradient $\nabla_{\theta}\pi(a | s)$ exists and its norm is bounded by a constant $G > 0$, i.e., $\|\nabla_{\theta}\pi(a | s)\| \leq G$.
- **L-smoothness:** There exists a constant $L > 0$ such that for all θ_1 and θ_2 , we have $\|\nabla J(\theta_1) - \nabla J(\theta_2)\| \leq L\|\theta_1 - \theta_2\|$.

Assumption 4 is commonly adopted in theoretical studies and is less restrictive than assumptions in related works [20]–[22]. It is satisfied by many practical parameterizations, such as general softmax and Gaussian policies. Under these conditions, we derive the following main convergence theorem. For a detailed proof, please see Appendix III.

Theorem 5 (Convergence bound): Suppose Assumption 4 and Assumption 1 (or Assumption 2 in the continuing cases) hold for episodic (or continuing) MDPs. Let $\delta^0 \triangleq J(\theta_*) - J(\theta_0)$ and choose a stepsize $0 < \eta \leq \frac{b}{L\bar{B}}$. Then for the iterates θ_t of the biased PG method in (5), we have

$$\frac{1}{T} \sum_{t=0}^{T-1} \|\nabla_{\theta}^e J(\theta_t)\|^2 \leq \frac{2\delta_0}{b\eta T} + \frac{2c}{(1 - \gamma)b} + \frac{L\eta C}{b},$$

where

$$b = \frac{\gamma^{m-1}(1 - \alpha)}{1 - \alpha\gamma^m}, \sigma = \frac{GR_{\max}|\mathcal{A}|}{1 - \gamma},$$

$$c = \left(1 - \frac{\gamma^{m-1}(1 - \alpha)}{1 - \alpha\gamma^m}\right)\sigma^2, B = b^2, C = \frac{c^2}{\sigma^2} + 2bc.$$

(or for continuing MDPs, $b = \frac{(1 - \gamma\beta)c_{\min}}{(1 - \gamma\beta)c_{\min} + 2(1 - \gamma)D}$, $c = \frac{2(1 - \gamma)D\sigma^2}{(1 - \gamma\beta)c_{\min} + 2(1 - \gamma)D}$).

Theorem 5 provides a finite-time convergence bound for the biased policy gradient method under mild conditions. The first term decays at a rate of $O(1/T)$, reflecting the standard convergence behavior. Theoretically, as γ approaches 1, the mismatch diminishes, causing b and B to converge to 1, while c and C tend to 0. As a result, the third term vanishes to 0 and the second term is bounded within a finite range. Theorem 5 partially explains the empirical observation in several earlier studies [8], [11], [12], where biased policy gradient methods exhibit performance comparable to their unbiased counterparts.

IV. NUMERICAL EXAMPLES

In this section, we provide numerical experiments to validate the global convergence results for tabular parameterizations. We investigate the behavior of biased policy gradient methods in the tabular parameterizations for continuing and episodic MDPs. For direct parameterizations, we utilize a projected gradient algorithm, where the updated policy is projected onto the feasible simplex region $\Delta^{|\mathcal{A}|}$ using a projection operator $P_{\Delta^{|\mathcal{A}|}}$, i.e., $\theta_{t+1} = P_{\Delta^{|\mathcal{A}|}}(\theta_t + \eta \hat{\nabla}_{\theta}^c J(\theta_t))$, where the gradient for direct parameterized policies is given in (6). For tabular softmax policies, the updates follow (5), with the corresponding gradient defined in (7).

Continuing MDPs: We adopt the Jack’s car rental problem [17, Example 4.2] as an illustrating example, where Jack moves cars between two rental locations for rentals to earn the most profit under the capacity limits. We set the maximum car capacity at each location to 5 cars, and at most 3 cars can be moved between locations in one day. To ensure that the actions are valid, if the action requests more cars to be moved than are available, only the available cars will be moved, and a penalty of \$30 per excess car will be charged. We compare the performance of the biased and unbiased policy gradient algorithms with varying γ , and the results of direct and tabular softmax parameterizations are given in Fig. 1 and Fig. 2, respectively.

Episodic MDPs: A gridworld example based on [17, Example 4.1] is utilized to illustrate the performance of tabular parameterizations in the episodic setting. In this example, an agent travels in a 4×4 gridworld with a state space $\mathcal{S} = \{1, \dots, 16\}$ and an action space $\mathcal{A} = \{\text{up, down, left, right}\}$. The environment contains two terminal states located at opposite corners, and the agent’s objective is to reach one of them using the shortest possible path. Each transition incurs a reward of -1 until a terminal state is reached. Moreover, the environment is affected by a northwest wind, introducing stochasticity: for any (s, a) , there is an additional probability of transitioning to the right or downward states, deviating from the intended action. Results of these two parameterizations are shown in Fig. 3 and Fig. 4.

Based on the results presented in Fig. 1–Fig. 4, we conclude the following: both the biased and unbiased policy gradient methods converge to the same optimal solution, albeit they have different convergence rates. This is consistent with our findings in Theorem 1 and Theorem 2, where we show

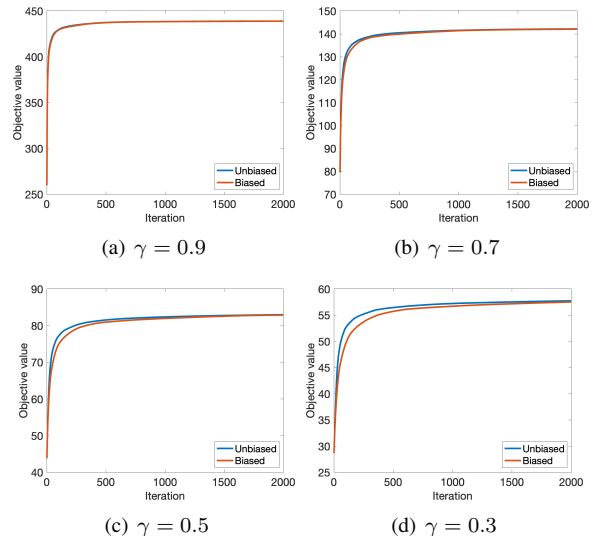


Fig. 1: Direct policy parameterization results for the Jack’s car rental problem under different choices of γ .

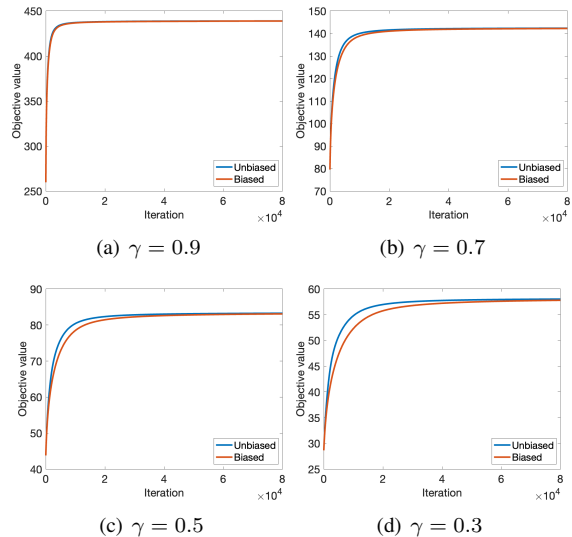


Fig. 2: Tabular softmax policy results for the Jack’s car rental problem under different choices of γ .

that both direct and softmax parameterizations converge to the global optimal solution. This demonstrates that even in the presence of a distribution mismatch, these parameterizations still lead to optimal outcomes. Furthermore, as the discount factor γ approaches 1, the performance of the biased and unbiased policy gradient methods become increasingly similar, converging at nearly the same rate. This observation further supports the theoretical results in Section III-B, which show that the mismatch is effectively eliminated when γ approaches 1.

V. CONCLUSION

We analyze the impact of the distribution mismatch on policy gradient methods for discounted MDPs. Specifically,

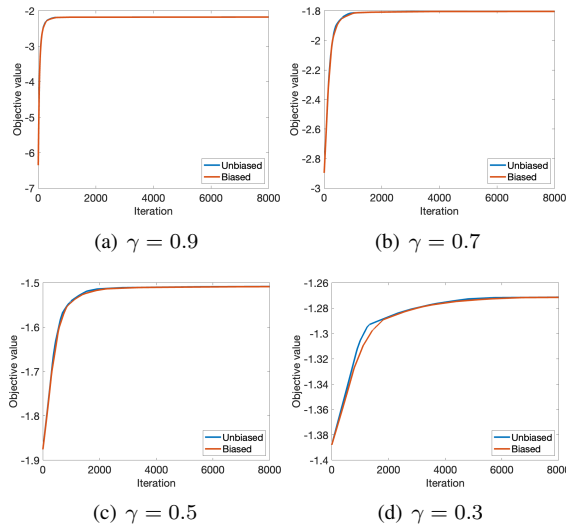


Fig. 3: Direct policy parameterization results for the grid-world problem under different choices of γ .

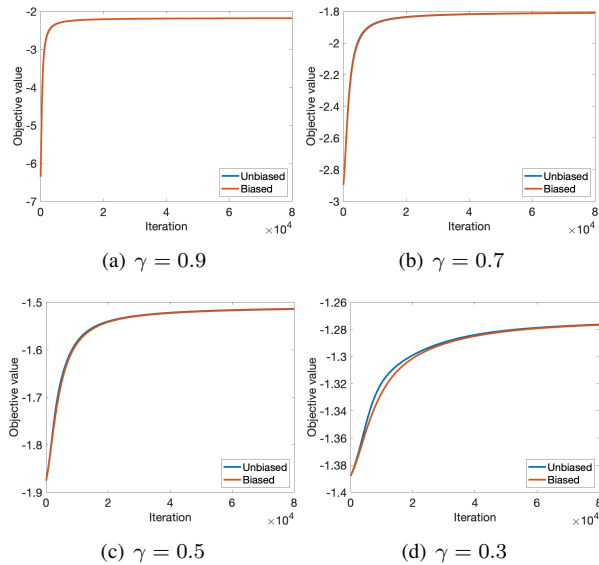


Fig. 4: Tabular softmax policy results for the gridworld problem under different choices of γ .

we show that despite the mismatch, both biased and unbiased policy gradient methods converge to the same solution under tabular parameterizations. We extend this analysis to more general parameterizations and derive theoretical bounds for the discrepancy between discounted and undiscounted distributions and derive a convergence bound. Finally, we verify our findings via several numerical experiments.

REFERENCES

- [1] J. Schulman, S. Levine, P. Abbeel, M. Jordan, and P. Moritz, “Trust region policy optimization,” in *Proceedings of International Conference on Machine Learning*, 2015, pp. 1889–1897.
- [2] V. Mnih, A. P. Badia, M. Mirza, A. Graves, T. Lillicrap, T. Harley, D. Silver, and K. Kavukcuoglu, “Asynchronous methods for deep reinforcement learning,” in *Proceedings of International Conference on Machine Learning*, 2016, pp. 1928–1937.
- [3] J. Schulman, P. Moritz, S. Levine, M. I. Jordan, and P. Abbeel, “High-dimensional continuous control using generalized advantage estimation,” in *Proceedings of International Conference on Learning Representations*, 2016.
- [4] J. Schulman, F. Wolski, P. Dhariwal, A. Radford, and O. Klimov, “Proximal policy optimization algorithms,” *arXiv preprint arXiv:1707.06347*, 2017.
- [5] T. Haarnoja, A. Zhou, P. Abbeel, and S. Levine, “Soft actor-critic: Off-policy maximum entropy deep reinforcement learning with a stochastic actor,” in *Proceedings of International Conference on Machine Learning*, 2018, pp. 1861–1870.
- [6] P. Thomas, “Bias in natural actor-critic algorithms,” in *Proceedings of International Conference on Machine Learning*, 2014, pp. 441–448.
- [7] C. Nota and P. S. Thomas, “Is the policy gradient a gradient?” in *Proceedings of the International Conference on Autonomous Agents and MultiAgent Systems*, 2020, p. 939–947.
- [8] S. Zhang, R. Laroche, H. van Seijen, S. Whiteson, and R. Tachet des Combes, “A deeper look at discounting mismatch in actor-critic algorithms,” in *Proceedings of International Conference on Autonomous Agents and Multiagent Systems*, 2022, p. 1491–1499.
- [9] S. Wu, L. Shi, J. Wang, and G. Tian, “Understanding policy gradient algorithms: A sensitivity-based approach,” in *Proceedings of International Conference on Machine Learning*, vol. 162, 2022, pp. 24 131–24 149.
- [10] S. Tosatto, A. Patterson, M. White, and R. Mahmood, “A temporal-difference approach to policy gradient estimation,” in *Proceedings of International Conference on Machine Learning*, vol. 162, 2022, pp. 21 609–21 632.
- [11] F. Che, G. Vasan, and A. R. Mahmood, “Correcting discount-factor mismatch in on-policy policy gradient methods,” in *Proceedings of International Conference on Machine Learning*, vol. 202, 2023, pp. 4218–4240.
- [12] H. Pan, D. Ye, X. Duan, Q. Fu, W. Yang, J. He, and M. Sun, “Revisiting estimation bias in policy gradients for deep reinforcement learning,” *arXiv preprint arXiv:2301.08442*, 2023.
- [13] S. Zhao, *Mathematical Foundations of Reinforcement Learning*. Springer Nature Press and Tsinghua University Press, 2025.
- [14] J. Mei, C. Xiao, C. Szepesvari, and D. Schuurmans, “On the global convergence rates of softmax policy gradient methods,” in *Proceedings of International Conference on Machine Learning*, 2020, pp. 6820–6829.
- [15] A. Agarwal, S. M. Kakade, J. D. Lee, and G. Mahajan, “On the theory of policy gradient methods: Optimality, approximation, and distribution shift,” *Journal of Machine Learning Research*, vol. 22, no. 98, pp. 1–76, 2021.
- [16] R. S. Sutton, D. McAllester, S. Singh, and Y. Mansour, “Policy gradient methods for reinforcement learning with function approximation,” in *Proceedings of Annual Conference on Neural Information Processing Systems*, 1999.
- [17] R. S. Sutton and A. G. Barto, *Reinforcement Learning: An Introduction*. Cambridge, MA, USA: A Bradford Book, 2018.
- [18] G. Li, Y. Wei, Y. Chi, Y. Gu, and Y. Chen, “Softmax policy gradient methods can take exponential time to converge,” in *Proceedings of Conference on Learning Theory*, 2021, pp. 3107–3110.
- [19] G. Lan, “Policy mirror descent for reinforcement learning: linear convergence, new sampling complexity, and generalized problem classes,” *Mathematical Programming*, vol. 198, no. 1, p. 1059–1106, 2022.
- [20] M. Papini, D. Binaghi, G. Canonaco, M. Pirotta, and M. Restelli, “Stochastic variance-reduced policy gradient,” in *Proceedings of International Conference on Machine Learning*, 2018, pp. 4026–4035.
- [21] K. Zhang, A. Koppel, H. Zhu, and T. Başar, “Global convergence of policy gradient methods to (almost) locally optimal policies,” *SIAM Journal on Control and Optimization*, vol. 58, no. 6, pp. 3586–3612, 2020.
- [22] S. Mu and D. Klabjan, “On the second-order convergence of biased policy gradient algorithms,” in *Proceedings of International Conference on Machine Learning*, 2024.
- [23] S. Kakade and J. Langford, “Approximately optimal approximate reinforcement learning,” in *Proceedings of International Conference on Machine Learning*, 2002, pp. 267–274.
- [24] D. A. Levin and Y. Peres, *Markov chains and mixing times*. American Mathematical Society, 2017.
- [25] Y. Demidovich, G. Malinovsky, I. Sokolov, and P. Richtárik, “A guide through the zoo of biased SGD,” in *Proceedings of Annual Conference on Neural Information Processing Systems*, 2024.

Outline of Appendix

- Appendix I: Proof of Section III-A
 - Appendix I.1: Proof of Theorem 1
 - Appendix I.2: Proof of Theorem 2
 - Appendix I.3: Examples of biased gradient with faster convergence speed
- Appendix II: Proof of Section III-B
 - Appendix II.1: Proof of Theorem 3
 - Appendix II.2: Proof of Theorem 4
- Appendix III: Proof of Section III-C
 - Appendix III.1: Proof of Theorem 5

Notation	Meaning
$J(\pi)$	Objective function for policy π .
$J(\theta)$	Equivalent to $J(\pi_\theta)$.
P^π	Transition matrix corresponding to policy π .
\tilde{P}^π	Principal minor of P^π restricted to the transient states. In episodic MDPs, \tilde{P}^π is a row-substochastic matrix.
d_0	Initial state distribution. $d_0(z) = 0$, for terminal state z ; $d_0(s) > 0$ for transient states.
\tilde{d}_0	$ \mathcal{S} - 1$ dimensional probability distribution vector over all transient states. $\tilde{d}_0^\top \mathbf{1} = 1$.
μ_π	Discounted state visitation counts. μ_π is not a valid probability distribution.
$d_{\pi,\gamma}$	Discounted state distribution. In continuing tasks, $d_{\pi,\gamma}$ is the normalized μ_π . In episodic tasks, $d_{\pi,\gamma}$ is obtained by setting $\mu_\pi(z) = 0$ and normalizing the modified μ_π . $d_{\pi,\gamma}$ is a valid probability distribution that is approximated in policy gradient by data sampling.
$\tilde{d}_{\pi,\gamma}$	Discounted state distributions over the transient states.
d_π	Undiscounted state distribution. In continuing tasks, d_π is the stationary distribution of P^π . In episodic tasks, $d_\pi(z) \triangleq 0$ for the terminal state z , while for transient states, the elements of d_π are proportional to the cumulative state visitation counts $\sum_{t=0}^{\infty} \mathbb{E}_{s_0 \sim d_0} [P^\pi(st = s s_0)]$, normalized to sum to 1.
\tilde{d}_π	Undiscounted state distributions over the transient states.
$\nabla_\theta J$	Gradient of $J(\theta)$.
$\nabla_\theta^c J$	Actual, theoretically correct policy gradient used in many popular algorithms.
$\tilde{\nabla}_\theta^c J$	Widely used biased version of $\nabla_\theta^c J$, which replaces the inaccessible distribution $d_{\pi,\gamma}$ with d_π .

TABLE I: Notation and their meanings

APPENDIX I
PROOF OF SECTION III-A

A. Proof of Theorem 1

We draw inspiration from the proof techniques presented in [15] and extend them to the case of biased undiscounted distributions. Since $\pi_\theta(a|s) = \theta_{s,a}$, we first give the specific expectation form of unbiased and biased policy gradient in direction parameterization case

$$(\nabla_\theta^c J)_{(s,a)} = d_{\pi,\gamma}(s)Q^\pi(s,a),$$

$$(\hat{\nabla}_\theta^c J)_{(s,a)} = d_\pi(s)Q^\pi(s,a).$$

Consider the performance difference lemma:

Lemma 1 (Performance difference lemma [23, Lemma 6.1]): Let $A^\pi(s,a)$ denote the advantage function of state-action pair (s,a) . For any policies π and $\tilde{\pi}$

$$J(\pi) - J(\tilde{\pi}) = \sum_s \mu_\pi(s) \sum_a \pi(a|s) [A^{\tilde{\pi}}(s,a)], \quad (12)$$

where μ_π is defined in (2). In continuing tasks, μ_π is the unnormalized version of $d_{\pi,\gamma}$, scaled by a constant factor of $\frac{1}{1-\gamma}$. In episodic tasks, the elements of μ_π corresponding to transient states are proportional to those of $d_{\pi,\gamma}$, scaled by a constant equal to $\frac{1}{1-\gamma} - \mu_\pi(z)$. Then we can rewrite the equation (12) as

$$J(\pi) - J(\tilde{\pi}) = \kappa \mathbb{E}_{s \sim d_{\pi,\gamma}, a \sim \pi(\cdot|s)} [A^{\tilde{\pi}}(s,a)].$$

In continuing tasks, $\kappa = \frac{1}{1-\gamma}$. In episodic tasks, κ is a scale value related to π . Following the proof technique for Lemma 4 in [15], let π_* denote an optimal solution corresponding to J^* . Then we have

$$\begin{aligned} & J^* - J(\pi) \\ &= \kappa \sum_{s,a} d_{\pi_*,\gamma}(s) \pi_*(a|s) A^\pi(s,a) \\ &\leq \kappa \sum_{s,a} d_{\pi_*,\gamma}(s) \max_{\bar{a}} A^\pi(s,\bar{a}) \\ &= \kappa \sum_s \frac{d_{\pi_*,\gamma}(s)}{d_\pi(s)} \cdot d_\pi(s) \max_{\bar{a}} A^\pi(s,\bar{a}) \\ &\leq \kappa \left\| \frac{d_{\pi_*,\gamma}}{d_\pi} \right\|_\infty \sum_s d_\pi(s) \max_{\bar{a}} A^\pi(s,\bar{a}) \quad (\max_{\bar{a}} A^\pi(s,\bar{a}) \geq 0) \\ &= \kappa \left\| \frac{d_{\pi_*,\gamma}}{d_\pi} \right\|_\infty \max_{\bar{\pi}} \sum_{s,a} d_\pi(s) \bar{\pi}(a|s) A^\pi(s,a) \\ &= \kappa \left\| \frac{d_{\pi_*,\gamma}}{d_\pi} \right\|_\infty \max_{\bar{\pi}} \sum_{s,a} d_\pi(s) (\bar{\pi}(a|s) - \pi(a|s)) A^\pi(s,a) \quad (\sum_a \pi(a|s) A^\pi(s,a) = 0) \\ &= \kappa \left\| \frac{d_{\pi_*,\gamma}}{d_\pi} \right\|_\infty \max_{\bar{\pi}} \sum_{s,a} d_\pi(s) (\bar{\pi}(a|s) - \pi(a|s)) Q^\pi(s,a) \quad (\sum_a (\bar{\pi}(a|s) - \pi(a|s)) V^\pi(s) = 0) \\ &= \kappa \left\| \frac{d_{\pi_*,\gamma}}{d_\pi} \right\|_\infty \max_{\bar{\pi}} (\bar{\pi} - \pi)^\top \hat{\nabla}_\theta^c J(\pi). \end{aligned}$$

B. Proof of Theorem 2

We first give the expectation gradient form of the tabular softmax parameterization.

$$\frac{\partial \pi(b|s')}{\partial \theta_{s,a}} = \begin{cases} 0, & \text{if } s' \neq s, \\ -\pi(a|s)\pi(b|s), & \text{if } s' = s, b \neq a, \\ \pi(a|s) - \pi(a|s)^2, & \text{if } s' = s, b = a. \end{cases}$$

Thus, we have

$$\begin{aligned}
(\nabla_{\theta}^e J)_{s,a} &= \mathbb{E}_{s' \sim d_{\pi,\gamma}} \left[\sum_b \pi(b|s') \frac{\partial \pi(b|s')}{\partial \theta_{s,a}} Q^{\pi}(s,a) \right] \\
&= d_{\pi,\gamma}(s) \left\{ - \sum_{b \neq a} \pi(a|s) \pi(b|s) Q^{\pi}(s,b) + [\pi(a|s) - \pi(a|s)^2] Q^{\pi}(s,a) \right\} \\
&= d_{\pi,\gamma}(s) \left\{ -\pi(a|s) \left[\sum_{b \in \mathcal{A}} \pi(b|s) Q^{\pi}(s,b) \right] + \pi(a|s) Q^{\pi}(s,a) \right\} \\
&= d_{\pi,\gamma}(s) \{ \pi(a|s) [Q^{\pi}(s,a) - V^{\pi}(s)] \} \\
&= d_{\pi,\gamma}(s) \pi(a|s) A^{\pi}(s,a).
\end{aligned}$$

Besides, the biased gradient is $(\hat{\nabla}_{\theta}^e J)_{s,a} = d_{\pi}(s) \pi(a|s) A^{\pi}(s,a)$.

The proof of Theorem 2 can be derived by adapting the global convergence argument for the unbiased gradient in Theorem 10 of [15]. In their analysis, the only properties of the discounted state distribution $d_{\pi,\gamma}$ that are required are $d_{\pi,\gamma}(s) > 0$ for all s and the fact that $d_{\pi,\gamma}$ is a valid probability distribution. These conditions also hold for the biased distributions d_{π} (in continuing MDPs) and \hat{d}_{π} (in episodic MDPs). Consequently, the key steps of the proof remain valid in the presence of distribution mismatch. Since a constant $\frac{1}{1-\gamma}$ should be absorbed into the stepsize, under tabular softmax parameterization and the same step size condition $\eta \leq (1-\gamma)^2/8$, the biased policy gradient also converges asymptotically to the global optimum.

C. Examples of biased gradient with faster convergence speed

We consider the gridworld example from [17, Example 4.1], which is also employed in Section IV. For convenience, a brief description is provided here: The gridworld is a 4×4 grid, where each cell represents a state, with $\mathcal{S} = \{1, \dots, 16\}$, and states 1 and 16 are terminal states. In each state, the agent can take one of four possible actions: $\mathcal{A} = \{\text{up, down, left, right}\}$. In the environment, a northwest wind is present, such that regardless of the agent's current state and chosen action, there is an additional ϵ probability of transitioning to the right and ϵ probability to the downward state, and a probability of $1-2\epsilon$ to move according to the intended action. The reward for all transitions is -1 until the terminal state is reached. The objective is to find the shortest path to one of the terminal states. We take $\epsilon = 0.1$ and for all nonterminal states s , the policy is $\pi(\text{up}|s) = \pi(\text{right}|s) = \frac{e^{\theta}}{2(1+e^{\theta})}$ and $\pi(\text{down}|s) = \pi(\text{left}|s) = \frac{1}{2(1+e^{\theta})}$.

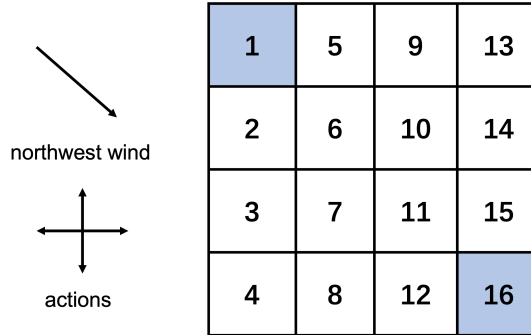


Fig. 5: Gridworld

We employ the unbiased PG update $\theta_{t+1} = \theta_t + \eta \nabla_{\theta}^e J(\theta_t)$ and the biased PG update $\theta_{t+1} = \theta_t + \eta \hat{\nabla}_{\theta}^e J(\theta_t)$ for varying discount factor γ . The results are shown in Fig. 6.

Based on the experimental results, under the certain incomplete parameterization in this problem, the biased algorithm not only converges to the same global solution as the unbiased method but also exhibits faster convergence. As γ approaches 1, the distribution mismatch diminishes, and the performance of the two algorithms becomes more similar.

This simple example demonstrates that despite the existence of distribution shift and the resulting theoretical gap, the biased policy gradient method can still perform excellently, and even outperform the unbiased method in practical implementations. Additionally, experiments in [8], [11], [12] show that their corrective methods do not always outperform the biased algorithm. This may help explain why the distribution mismatch remains unresolved in many practical state-of-the-art algorithms.

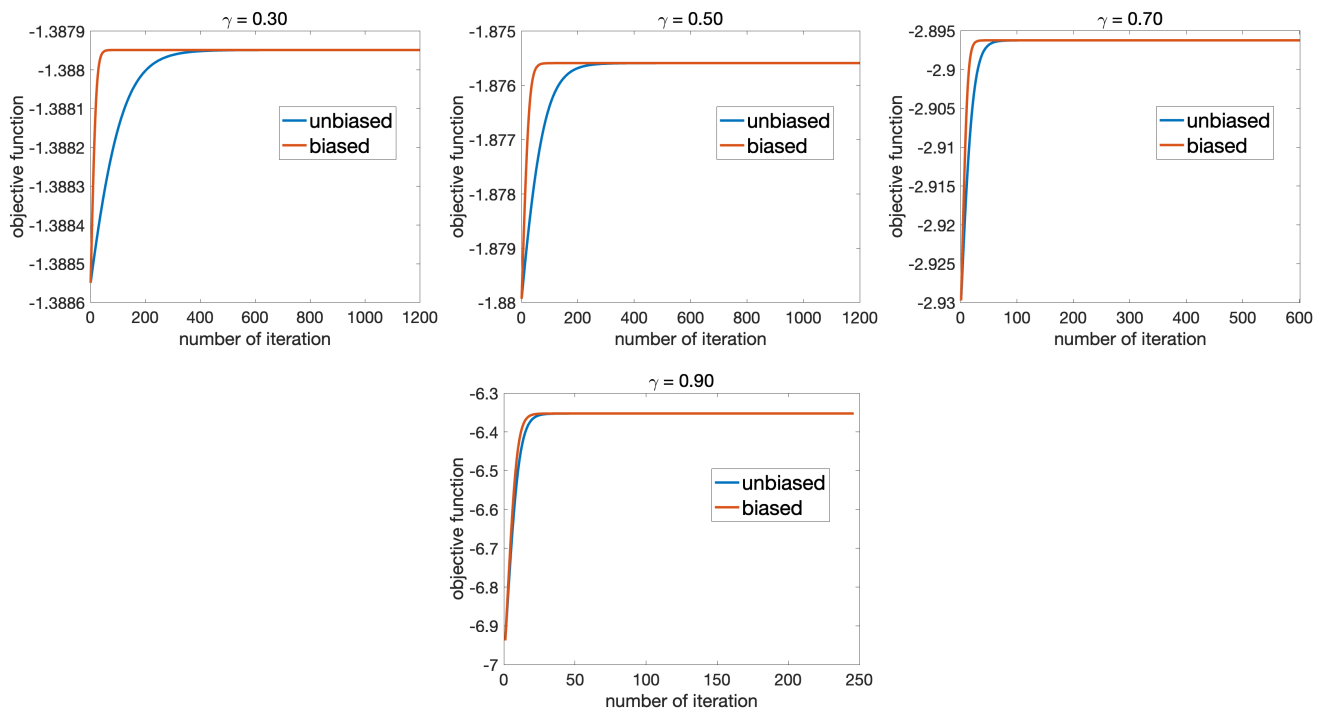


Fig. 6: Results of biased and unbiased PG algorithms with certain parameterizations for gridworld problems under different γ .

APPENDIX II
PROOF OF SECTION III-B

A. Proof of Theorem 3

For an episodic MDP, we assume that under no matter what policy, the agent reaches the absorbing state z with a positive probability:

(Absorbing probability assumption) There exist an integer $m > 0$ and a positive real number $\alpha < 1$ such that

$$\mathbb{P}(s_m \neq z \mid s_0, \pi) \leq \alpha, \quad \forall s_0 \in \mathcal{S}, \pi.$$

Thus we have

$$(\tilde{P}^\pi)^m \mathbf{1} \leq \alpha \mathbf{1},$$

and for any $k = 0, 1, \dots$

$$\sum_{t=km}^{(k+1)m-1} \gamma^t (\tilde{P}^\pi)^t \mathbf{1} \leq \alpha^k \frac{\gamma^{km}(1-\gamma^m)}{1-\gamma} \mathbf{1}.$$

For any basic vector e_i , where all elements except the i -th are zero and the i -th element is one, we have the same result:

$$(\tilde{P}^\pi)^m e_i \leq \alpha \mathbf{1},$$

$$\sum_{t=km}^{(k+1)m-1} (\tilde{P}^\pi)^t e_i \leq m\alpha^k \mathbf{1}.$$

Without loss of generality, we assume $d_0(z) = 0$. If this is not the case, it can be adjusted to zero by redistributing its probability mass among the remaining elements and normalizing. This modification would result in the objective function of all policies being scaled by a constant factor, without affecting the relative comparisons between them. Then the distribution \tilde{d}_0 is a valid distribution with $\tilde{d}_0^\top \mathbf{1} = 1$. The matrix form of $\tilde{d}_{\pi, \gamma}$ and \tilde{d}_π can be written as

$$\begin{aligned} \tilde{d}_{\pi, \gamma}^\top &= \frac{\sum_{t=0}^{\infty} \gamma^t \tilde{d}_0^\top (\tilde{P}^\pi)^t}{\sum_{t=0}^{\infty} \gamma^t \tilde{d}_0^\top (\tilde{P}^\pi)^t \mathbf{1}} = \frac{\tilde{d}_0^\top (I - \gamma \tilde{P}^\pi)^{-1}}{\tilde{d}_0^\top (I - \gamma \tilde{P}^\pi)^{-1} \mathbf{1}}, \\ \tilde{d}_\pi^\top &= \frac{\sum_{t=0}^{\infty} \tilde{d}_0^\top (\tilde{P}^\pi)^t}{\sum_{t=0}^{\infty} \tilde{d}_0^\top (\tilde{P}^\pi)^t \mathbf{1}} = \frac{\tilde{d}_0^\top (I - \tilde{P}^\pi)^{-1}}{\tilde{d}_0^\top (I - \tilde{P}^\pi)^{-1} \mathbf{1}}. \end{aligned} \tag{13}$$

Note that since \tilde{P}^π is row-sub stochastic, $I - \tilde{P}^\pi$ is nonsingular. Then we have

$$\left\| \frac{\tilde{d}_{\pi, \gamma}}{\tilde{d}_\pi} \right\|_\infty = \underbrace{\frac{\tilde{d}_0^\top (I - \tilde{P}^\pi)^{-1} \mathbf{1}}{\tilde{d}_0^\top (I - \gamma \tilde{P}^\pi)^{-1} \mathbf{1}}}_I \underbrace{\left\| \frac{\tilde{d}_0^\top (I - \gamma \tilde{P}^\pi)^{-1}}{\tilde{d}_0^\top (I - \tilde{P}^\pi)^{-1}} \right\|_\infty}_{II}.$$

For item II, it is monotonically increasing with respect to γ and thus we have it less than or equal to 1.

For item I, first we give a bound for $\frac{\tilde{d}_0^\top (I - \tilde{P}^\pi)^{-1} (I - \gamma \tilde{P}^\pi)^{-1} \mathbf{1}}{\tilde{d}_0^\top (I - \tilde{P}^\pi)^{-1} \mathbf{1}}$, which is useful in the following proof. According to the Hölder's inequality, we have

$$\begin{aligned} \frac{\tilde{d}_0^\top (I - \tilde{P}^\pi)^{-1} (I - \gamma \tilde{P}^\pi)^{-1} \mathbf{1}}{\tilde{d}_0^\top (I - \tilde{P}^\pi)^{-1} \mathbf{1}} &\leq \frac{\|\tilde{d}_0^\top (I - \tilde{P}^\pi)^{-1}\|_1 \|(I - \gamma \tilde{P}^\pi)^{-1} \mathbf{1}\|_\infty}{\tilde{d}_0^\top (I - \tilde{P}^\pi)^{-1} \mathbf{1}} \\ &= \|(I - \gamma \tilde{P}^\pi)^{-1} \mathbf{1}\|_\infty \\ &= \left\| \sum_{k=0}^{\infty} \sum_{t=km}^{(k+1)m-1} \gamma^t (\tilde{P}^\pi)^t \mathbf{1} \right\|_\infty \\ &\leq \left\| \sum_{k=0}^{\infty} \alpha^k \frac{\gamma^{km}(1-\gamma^m)}{1-\gamma} \mathbf{1} \right\|_\infty \\ &= \frac{1-\gamma^m}{(1-\gamma)(1-\alpha\gamma^m)}. \end{aligned}$$

Note that according to the Woodbury matrix identity theory, we have

$$\begin{aligned}
(I - \gamma \tilde{P}^\pi)^{-1} &= \left[(1 - \gamma)I + \gamma(I - \tilde{P}^\pi) \right]^{-1} \\
&= \frac{1}{\gamma} (I - \tilde{P}^\pi)^{-1} - \frac{1}{\gamma} (I - \tilde{P}^\pi)^{-1} \left[\frac{\gamma}{1 - \gamma} (I - \tilde{P}^\pi) + I \right]^{-1} \\
&= \frac{1}{\gamma} (I - \tilde{P}^\pi)^{-1} - \frac{1 - \gamma}{\gamma} (I - \tilde{P}^\pi)^{-1} (I - \gamma \tilde{P}^\pi)^{-1}.
\end{aligned}$$

Then we derive that

$$\begin{aligned}
\frac{\tilde{d}_0^\top (I - \tilde{P}^\pi)^{-1} \mathbb{1}}{\tilde{d}_0^\top (I - \gamma \tilde{P}^\pi)^{-1} \mathbb{1}} &= \frac{1}{\frac{1}{\gamma} - \frac{1 - \gamma}{\gamma} \frac{\tilde{d}_0^\top (I - \tilde{P}^\pi)^{-1} (I - \gamma \tilde{P}^\pi)^{-1} \mathbb{1}}{\tilde{d}_0^\top (I - \tilde{P}^\pi)^{-1} \mathbb{1}}} \\
&\leq \frac{1}{\frac{1}{\gamma} - \frac{1 - \gamma}{\gamma} \frac{1 - \gamma^m}{(1 - \gamma)(1 - \alpha \gamma^m)}} \\
&= \frac{1 - \alpha \gamma^m}{\gamma^{m-1} (1 - \alpha)}.
\end{aligned}$$

Consequently, we have

$$\left\| \frac{\tilde{d}_{\pi, \gamma}}{\tilde{d}_\pi} \right\|_\infty \leq \frac{1 - \alpha \gamma^m}{\gamma^{m-1} (1 - \alpha)}.$$

As for the second bound, note that

$$\left\| \frac{\tilde{d}_\pi}{\tilde{d}_{\pi, \gamma}} \right\|_\infty = \underbrace{\frac{\tilde{d}_0^\top (I - \gamma \tilde{P}^\pi)^{-1} \mathbb{1}}{\tilde{d}_0^\top (I - \tilde{P}^\pi)^{-1} \mathbb{1}}}_I \underbrace{\left\| \frac{\tilde{d}_0^\top (I - \tilde{P}^\pi)^{-1}}{\tilde{d}_0^\top (I - \gamma \tilde{P}^\pi)^{-1}} \right\|_\infty}_{II}.$$

For term I, it is monotonically increasing with respect to γ and thus we have it less than or equal to 1. For term II, we still use the Woodbury matrix identity formula and obtain:

$$\begin{aligned}
(I - \tilde{P}^\pi)^{-1} &= \gamma \left[I - \gamma \tilde{P}^\pi - (1 - \gamma)I \right]^{-1} \\
&= \gamma \left[(I - \gamma \tilde{P}^\pi)^{-1} - (I - \gamma \tilde{P}^\pi)^{-1} \left(-\frac{1}{1 - \gamma} (I - \gamma \tilde{P}^\pi) + I \right)^{-1} \right] \\
&= \gamma (I - \gamma \tilde{P}^\pi)^{-1} + (1 - \gamma) (I - \gamma \tilde{P}^\pi)^{-1} (I - \tilde{P}^\pi)^{-1}.
\end{aligned}$$

Thus, we have

$$\left\| \frac{\tilde{d}_0^\top (I - \tilde{P}^\pi)^{-1}}{\tilde{d}_0^\top (I - \gamma \tilde{P}^\pi)^{-1}} \right\|_\infty = \gamma + (1 - \gamma) \left\| \frac{\tilde{d}_0^\top (I - \gamma \tilde{P}^\pi)^{-1} (I - \tilde{P}^\pi)^{-1}}{\tilde{d}_0^\top (I - \gamma \tilde{P}^\pi)^{-1}} \right\|_\infty.$$

We calculate that

$$\frac{\tilde{d}_0^\top (I - \gamma \tilde{P}^\pi)^{-1} (I - \tilde{P}^\pi)^{-1} \mathbf{e}_i}{\tilde{d}_0^\top (I - \gamma \tilde{P}^\pi)^{-1} \mathbf{e}_i} \leq \frac{\left\| \tilde{d}_0^\top (I - \gamma \tilde{P}^\pi)^{-1} \right\|_1 \left\| (I - \tilde{P}^\pi)^{-1} \mathbf{e}_i \right\|_\infty}{\tilde{d}_0^\top \mathbf{e}_i}.$$

Consider

$$\begin{aligned}
\left\| \tilde{d}_0^\top (I - \gamma \tilde{P}^\pi)^{-1} \right\|_1 &= \tilde{d}_0^\top (I - \gamma \tilde{P}^\pi)^{-1} \mathbb{1} \\
&\leq \tilde{d}_0^\top \frac{1 - \gamma^m}{(1 - \gamma)(1 - \alpha \gamma^m)} \mathbb{1} \\
&= \frac{1 - \gamma^m}{(1 - \gamma)(1 - \alpha \gamma^m)}.
\end{aligned}$$

Besides, we have

$$\left\| (I - \tilde{P}^\pi)^{-1} \mathbf{e}_i \right\|_\infty = \left\| \sum_{k=0}^{\infty} \sum_{t=km}^{(k+1)m-1} (\tilde{P}^\pi)^t \mathbf{e}_i \right\|_\infty \leq \left\| \sum_{k=0}^{\infty} m \alpha^k \mathbb{1} \right\|_\infty = \frac{m}{1 - \alpha}.$$

Furthermore,

$$\left\| \frac{\tilde{d}_0^\top (I - \gamma \tilde{P}^\pi)^{-1} (I - \tilde{P}^\pi)^{-1}}{\tilde{d}_0^\top (I - \gamma \tilde{P}^\pi)^{-1}} \right\|_\infty = \max_i \frac{\tilde{d}_0^\top (I - \gamma \tilde{P}^\pi)^{-1} (I - \tilde{P}^\pi)^{-1} \mathbf{e}_i}{\tilde{d}_0^\top (I - \gamma \tilde{P}^\pi)^{-1} \mathbf{e}_i}.$$

Consequently, we obtain

$$\left\| \frac{\tilde{d}_\pi}{\tilde{d}_{\pi, \gamma}} \right\|_\infty \leq \gamma + \frac{m(1 - \gamma^m)}{(1 - \alpha)(1 - \alpha\gamma^m) \min_s d_0(s)}.$$

B. Proof of Theorem 4

For continuing MDP, we introduce the following assumption to ensure the Markov chain exhibits stable long-term behavior:
(Ergodicity Assumption) Given any π , the corresponding Markov chain P^π is ergodic.

This assumption means P^π is irreducible and aperiodic, ensuring the existence of a unique stationary distribution d_π . Besides, it guarantees all elements in d_π is positive, i.e., $\min_s d_\pi(s) > 0$. Next, we introduce the definition of total variation distance.

Definition 1 (Total variation distance): Given two probability distributions μ and ν on \mathcal{X} , the total variation distance is defined by

$$\|\mu - \nu\|_{\text{TV}} = \max_{A \subset \mathcal{X}} |\mu(A) - \nu(A)|.$$

On discrete domains, this can be calculated by

$$\|\mu - \nu\|_{\text{TV}} = \frac{1}{2} \sum_{x \in \mathcal{X}} |\mu(x) - \nu(x)|.$$

Then a useful theorem is introduced for the following proof.

Theorem 6 (Convergence Theorem [24, Theorem 4.9]): Suppose that a Markov chain P is irreducible and aperiodic, with stationary distribution d_π . Then there exist constants $\beta \in (0, 1)$ and $D > 0$ such that

$$\max_{x \in \mathcal{X}} \|P^t(x, \cdot) - d_\pi\|_{\text{TV}} \leq D\beta^t. \quad (14)$$

Specific to our problem, there exist constants $\beta \in (0, 1)$ and $D > 0$ such that

$$\max_{s \in \mathcal{S}} \|(P^\pi)^t(s, \cdot) - d_\pi\|_{\text{TV}} \leq D\beta^t.$$

Then we have

$$\begin{aligned} \|d_0^\top (P^\pi)^t - d_\pi\|_{\text{TV}} &= \left\| \sum_s d_0(s) (P^\pi)^t(s, \cdot) - d_\pi \right\|_{\text{TV}} \\ &= \left\| \sum_s d_0(s) ((P^\pi)^t(s, \cdot) - d_\pi) \right\|_{\text{TV}} \\ &\leq \sum_s d_0(s) \|(P^\pi)^t(s, \cdot) - d_\pi\|_{\text{TV}} \\ &\leq \max_{s \in \mathcal{S}} \|(P^\pi)^t(s, \cdot) - d_\pi\|_{\text{TV}} \\ &\leq D\beta^t. \end{aligned}$$

Considering the definition of the total variation distance, for any $s \in \mathcal{S}$,

$$|(d_0^\top (P^\pi)^t)(s) - d_\pi(s)| \leq 2 \|d_0^\top (P^\pi)^t - d_\pi\|_{\text{TV}} \leq 2D\beta^t.$$

Thus, we have the following pointwise inequality:

$$\begin{aligned} d_0^\top P^t &\leq d_\pi^\top + 2D\beta^t \mathbf{1}^\top, \\ d_\pi^\top &\leq d_0^\top P^t + 2D\beta^t \mathbf{1}^\top. \end{aligned}$$

In the continuing MDP, the discounted distribution can be expressed in the following expression:

$$d_{\pi, \gamma}^\top = \frac{\sum_{t=0}^{\infty} \gamma^t d_0^\top (P^\pi)^t}{\sum_{t=0}^{\infty} \gamma^t d_0^\top (P^\pi)^t \mathbf{1}} = (1 - \gamma) d_0^\top (I - \gamma P^\pi)^{-1}.$$

Since $d_0 > 0$, it is guaranteed that $d_{\pi,\gamma} \geq (1 - \gamma)d_0 > 0$, and thus $\min_s d_{\pi,\gamma}(s) > 0$. Then we have

$$\begin{aligned}
\left\| \frac{d_{\pi,\gamma}}{d_\pi} \right\|_\infty &= \left\| \frac{(1 - \gamma) \sum_{t=0}^{\infty} \gamma^t d_0^\top (P^\pi)^t}{d_\pi^\top} \right\|_\infty \\
&\leq 1 + (1 - \gamma) \left\| \frac{2D \sum_{t=0}^{\infty} \gamma^t \beta^t \mathbf{1}}{d_\pi} \right\|_\infty \\
&\leq 1 + \frac{2(1 - \gamma)D}{(1 - \gamma\beta) \min_s d_\pi(s)} \\
&\leq 1 + \frac{2(1 - \gamma)D}{(1 - \gamma\beta)c_{\min}}, \\
\left\| \frac{d_\pi}{d_{\pi,\gamma}} \right\|_\infty &= \left\| \frac{(1 - \gamma) \sum_{t=0}^{\infty} \gamma^t d_\pi}{d_{\pi,\gamma}^\top} \right\|_\infty \\
&\leq 1 + (1 - \gamma) \left\| \frac{2D \sum_{t=0}^{\infty} \gamma^t \beta^t \mathbf{1}}{d_{\pi,\gamma}} \right\|_\infty \\
&\leq 1 + \frac{2(1 - \gamma)D}{(1 - \gamma\beta) \min_s d_{\pi,\gamma}(s)} \\
&\leq 1 + \frac{2(1 - \gamma)D}{(1 - \gamma\beta)c_{\min,\gamma}}.
\end{aligned}$$

APPENDIX III
PROOF OF SECTION III-C

A. Proof of Theorem 5

Our analysis is inspired by the performance bound of a biased stochastic estimator under the biased ABC assumption, as established in [25, Theorem 3]. However, since a direct application of that result is not applicable in our setting, we provide a detailed proof here. We first establish that the algorithm satisfies the following assumption:

Assumption 5 (Biased ABC): Supposing Assumption 4 and Assumption 1 (or Assumption 2 in the continuing cases) hold for episodic (or continuing) MDPs, we have

$$\begin{aligned}\langle \nabla_{\theta}^e J, \hat{\nabla}_{\theta}^e J \rangle &\geq b \|\nabla_{\theta}^e J\|^2 - c, \\ \|\hat{\nabla}_{\theta}^e J\|^2 &\leq B \|\nabla_{\theta}^e J\|^2 + C,\end{aligned}$$

where

$$\begin{aligned}b &= \frac{\gamma^{m-1}(1-\alpha)}{1-\alpha\gamma^m}, \sigma = \frac{GR_{\max}|\mathcal{A}|}{1-\gamma}, \\ c &= \left(1 - \frac{\gamma^{m-1}(1-\alpha)}{1-\alpha\gamma^m}\right)\sigma^2, B = b^2, C = \frac{c^2}{\sigma^2} + 2bc.\end{aligned}$$

(or for continuing MDPs, $b = \frac{(1-\gamma\beta)c_{\min}}{(1-\gamma\beta)c_{\min}+2(1-\gamma)D}$, $c = \frac{2(1-\gamma)D\sigma^2}{(1-\gamma\beta)c_{\min}+2(1-\gamma)D}$.)

First, since the rewards are bounded, i.e., $R(s, a) \in [-R_{\max}, R_{\max}]$, it follows from the definition of the state-action value function that for any $(s, a) \in \mathcal{S} \times \mathcal{A}$, we have

$$|Q(s, a)| = \left| \mathbb{E} \left[\sum_{t=0}^{\infty} \gamma^t R_t \mid S_0 = s, A_0 = a \right] \right| \leq \frac{R_{\max}}{1-\gamma}.$$

Moreover, since the policy gradient is bounded, define $g(s) \triangleq \sum_{a \in \mathcal{A}} \nabla_{\theta} \pi(a \mid s) Q(s, a)$ and it holds that

$$\begin{aligned}\|g(s)\| &= \left\| \sum_{a \in \mathcal{A}} \nabla_{\theta} \pi(a \mid s) Q(s, a) \right\| \leq \frac{GR_{\max}|\mathcal{A}|}{1-\gamma} \triangleq \sigma, \\ \|\nabla_{\theta}^e J\| &= \left\| \sum_s d_{\pi, \gamma}(s) g(s) \right\| \leq \sigma.\end{aligned}$$

We calculate that

$$\begin{aligned}\langle \nabla_{\theta}^e J, \hat{\nabla}_{\theta}^e J \rangle &= \left\langle \sum_s d_{\pi, \gamma}(s) g(s), \sum_s d_{\pi}(s) g(s) \right\rangle \\ &= \left\langle \sum_s d_{\pi, \gamma}(s) g(s), \sum_s \left\| \frac{d_{\pi, \gamma}}{d_{\pi}} \right\|_{\infty}^{-1} d_{\pi, \gamma}(s) g(s) \right\rangle \\ &\quad + \left\langle \sum_s d_{\pi, \gamma}(s) g(s), \sum_s \left(d_{\pi}(s) - \left\| \frac{d_{\pi, \gamma}}{d_{\pi}} \right\|_{\infty}^{-1} d_{\pi, \gamma}(s) \right) g(s) \right\rangle \\ &= \left\| \frac{d_{\pi, \gamma}}{d_{\pi}} \right\|_{\infty}^{-1} \|\nabla_{\theta}^e J\|^2 + \left\langle \sum_s d_{\pi, \gamma}(s) g(s), \sum_s \left(d_{\pi}(s) - \left\| \frac{d_{\pi, \gamma}}{d_{\pi}} \right\|_{\infty}^{-1} d_{\pi, \gamma}(s) \right) g(s) \right\rangle.\end{aligned}$$

Consider the second term of the above equation:

$$\begin{aligned}&\left\langle \sum_s d_{\pi, \gamma}(s) g(s), \sum_s \left(d_{\pi}(s) - \left\| \frac{d_{\pi, \gamma}}{d_{\pi}} \right\|_{\infty}^{-1} d_{\pi, \gamma}(s) \right) g(s) \right\rangle \\ &= \sum_{s_1} d_{\pi, \gamma}(s_1) \sum_{s_2} \left(d_{\pi}(s_2) - \left\| \frac{d_{\pi, \gamma}}{d_{\pi}} \right\|_{\infty}^{-1} d_{\pi, \gamma}(s_2) \right) \langle g(s_1), g(s_2) \rangle \\ &\geq - \sum_{s_1} d_{\pi, \gamma}(s_1) \sum_{s_2} \left(d_{\pi}(s_2) - \left\| \frac{d_{\pi, \gamma}}{d_{\pi}} \right\|_{\infty}^{-1} d_{\pi, \gamma}(s_2) \right) \sigma^2 \\ &= -(1 - \left\| \frac{d_{\pi, \gamma}}{d_{\pi}} \right\|_{\infty}^{-1}) \sigma^2,\end{aligned}$$

where we consider the pointwise positiveness of $d_\pi - \left\| \frac{d_{\pi,\gamma}}{d_\pi} \right\|_\infty^{-1} d_{\pi,\gamma}$ in the third line. Thus, we have

$$\langle \nabla_\theta^e J, \hat{\nabla}_\theta^e J \rangle \geq \left\| \frac{d_{\pi,\gamma}}{d_\pi} \right\|_\infty^{-1} \|\nabla_\theta^e J\|^2 - \left(1 - \left\| \frac{d_{\pi,\gamma}}{d_\pi} \right\|_\infty^{-1}\right) \sigma^2$$

In the episodic MDPs, the above process remains the same expect $d_{\pi,\gamma}$ and d_π are replaced by $\tilde{d}_{\pi,\gamma}$ and \tilde{d}_π . Considering the upper bounds for $\left\| \frac{\tilde{d}_{\pi,\gamma}}{\tilde{d}_\pi} \right\|_\infty$ given by Theorem 3 for episodic MDPS (or upper bounds for $\left\| \frac{d_{\pi,\gamma}}{d_\pi} \right\|_\infty$ in Theorem 4 under the continuing setting), when $b = \frac{\gamma^{m-1}(1-\alpha)}{1-\alpha\gamma^m}$, $c = (1 - \frac{\gamma^{m-1}(1-\alpha)}{1-\alpha\gamma^m})\sigma^2$ (or $b = \frac{(1-\gamma\beta)c_{\min}}{(1-\gamma\beta)c_{\min}+2(1-\gamma)D}$, $c = \frac{2(1-\gamma)D\sigma^2}{(1-\gamma\beta)c_{\min}+2(1-\gamma)D}$ for continuing MDPs), we have

$$\langle \nabla_\theta^e J, \hat{\nabla}_\theta^e J \rangle \geq b \|\nabla_\theta^e J\|^2 - c,$$

where the first condition in Assumption 5 is satisfied.

As for the norm of $\hat{\nabla}_\theta^e J$, we have

$$\begin{aligned} \|\hat{\nabla}_\theta^e J\|^2 &= \langle \hat{\nabla}_\theta^e J, \hat{\nabla}_\theta^e J \rangle \\ &= \left\langle \sum_s \left[\left\| \frac{d_{\pi,\gamma}}{d_\pi} \right\|_\infty^{-1} d_{\pi,\gamma}(s) + \left(d_\pi(s) - \left\| \frac{d_{\pi,\gamma}}{d_\pi} \right\|_\infty^{-1} d_{\pi,\gamma}(s) \right) \right] g(s), \right. \\ &\quad \left. + \sum_s \left[\left\| \frac{d_{\pi,\gamma}}{d_\pi} \right\|_\infty^{-1} d_{\pi,\gamma}(s) + \left(d_\pi(s) - \left\| \frac{d_{\pi,\gamma}}{d_\pi} \right\|_\infty^{-1} d_{\pi,\gamma}(s) \right) \right] g(s) \right\rangle \\ &\leq \left\| \frac{d_{\pi,\gamma}}{d_\pi} \right\|_\infty^{-2} \|\nabla_\theta^e J\|^2 + \left[\left(1 - \left\| \frac{d_{\pi,\gamma}}{d_\pi} \right\|_\infty^{-1}\right)^2 \sigma^2 + 2 \left\| \frac{d_{\pi,\gamma}}{d_\pi} \right\|_\infty^{-1} \left(1 - \left\| \frac{d_{\pi,\gamma}}{d_\pi} \right\|_\infty^{-1}\right) \sigma^2 \right]. \end{aligned}$$

When taking $B = b^2$, $C = \frac{c^2}{\sigma^2} + 2bc$, we have

$$\|\hat{\nabla}_\theta^e J\|^2 \leq B \|\nabla_\theta^e J\|^2 + C,$$

and the second condition in Assumption 5 is satisfied.

A key distinction between our setting and [25] lies in the fact that, while their analysis relies on the theoretical gradient $\nabla_\theta J$ of the objective function J , our setting involves an empirical gradient $\nabla_\theta^e J$ that differs from $\nabla_\theta J$ by a proportionality constant. Consequently, the general biased ABC analysis is not directly applicable, and we provide a complete proof tailored to our setting. We suppose $\nabla_\theta J = K_\theta \nabla_\theta^e J$, where in continuing setting, $K_\theta = \frac{1}{1-\gamma}$ while in episodic setting, $K_\theta = \frac{1}{1-\gamma} - \mu^\pi(z)$. Since $d_0(z) = 0$, we have $\mu^\pi(z) = \sum_{t=0}^{\infty} \mathbb{E}_{s_0 \sim d_0} \gamma^t [P^\pi(s_t = z | s_0)] = \sum_{t=1}^{\infty} \mathbb{E}_{s_0 \sim d_0} \gamma^t [P^\pi(s_t = z | s_0)] \leq \frac{\gamma}{1-\gamma}$. Then for episodic setting, $1 \leq K_\theta < \frac{1}{1-\gamma}$. Consequently, for whatever setting, we have $1 \leq K_\theta \leq \frac{1}{1-\gamma}$.

We now proceed to the proof of Theorem 5. Recall the practical biased gradient algorithm in (5), $\theta_{t+1} = \theta_t + \eta \hat{\nabla}_\theta^e J(\theta_t)$. Under the L -smoothness condition specified in Assumption 4, we have

$$\begin{aligned} J(\theta_{t+1}) &\geq J(\theta_t) + \langle \nabla_\theta J(\theta_t), \theta_{t+1} - \theta_t \rangle - \frac{L}{2} \|\theta_{t+1} - \theta_t\|^2 \\ &= J(\theta_t) + \eta K_{\theta_t} \langle \nabla_\theta^e J(\theta_t), \hat{\nabla}_\theta^e J(\theta_t) \rangle - \frac{L\eta^2}{2} \|\hat{\nabla}_\theta^e J(\theta_t)\|^2 \\ &\geq J(\theta_t) + \eta K_{\theta_t} b \|\nabla_\theta J\|^2 - \eta K_{\theta_t} c - \frac{L\eta^2 B}{2} \|\nabla_\theta J\|^2 - \frac{L\eta^2 C}{2} \\ &\geq J(\theta_t) + \left(\eta b - \frac{L\eta^2 B}{2} \right) \|\nabla_\theta J\|^2 - \frac{\eta c}{1-\gamma} - \frac{L\eta^2 C}{2}, \end{aligned}$$

where the ABC assumption in Assumption 5 is used in the third line. Subtracting $J(\theta_*)$ from both sides and defining $\delta_t \triangleq J(\theta_*) - J(\theta_t)$ and $r_t \triangleq \|\nabla_\theta^e J(\theta_t)\|^2$ give

$$\left(\eta b - \frac{L\eta^2 B}{2} \right) r_t \leq \delta_t - \delta_{t+1} + \frac{\eta c}{1-\gamma} + \frac{L\eta^2 C}{2}.$$

Summing over $t = 0, \dots, T-1$ and dividing T , we obtain

$$\left(\eta b - \frac{L\eta^2 B}{2} \right) \frac{\sum_{t=0}^{T-1} r_t}{T} \leq \frac{\delta_0 - \delta_T}{T} + \frac{\eta c}{1-\gamma} + \frac{L\eta^2 C}{2} \leq \frac{\delta_0}{T} + \frac{\eta c}{1-\gamma} + \frac{L\eta^2 C}{2}.$$

Since the stepszie η satisfies $0 < \eta \leq \frac{b}{LB}$, we have $b - \frac{L\eta B}{2} \geq \frac{b}{2}$ and thus

$$\frac{1}{T} \sum_{t=0}^{T-1} \|\nabla_\theta^e J(\theta_t)\|^2 \leq \frac{2\delta_0}{b\eta T} + \frac{2c}{(1-\gamma)b} + \frac{L\eta C}{b}.$$